Catalytic acetalization of carbonyl compounds over cation (Ce3+, Fe3+ and Al3+) exchanged montmorillonites and Ce3+-exchanged Y zeolites

Bejoy Thomas, Vasanthakumar Ganga Ramu, Sanjay Gopinath, Jino George,
Manju Kurian, Guillaume Laurent, Glenna L. Drisko, Sankaran Sugunan

Research Paper

Catalytic acetalization of carbonyl compounds over cation (Ce^{3+}, Fe^{3+} and Al^{3+}) exchanged montmorillonites and Ce^{3+}-exchanged Y zeolites

Bejoy Thomas [a,b,*], Vasanthakumar Ganga Ramu [c], Sanjay Gopinath [a], Jino George [a], Manju Kurian [d], Guillaume Laurent [b], Glenna L. Drisko [b], Sankaran Sugunan [a]

[a] *Department of Applied Chemistry, Cochin University of Science and Technology, Kochi-682 022, India*
[b] *University Pierre et Marie Curie, Univ. Paris 06, CNRS, Laboratoire de Chimie de la Matière Condensée de Paris, Collège de France, 11 place Marcellin Berthelot, 75005 Paris, France*
[c] *Organic Chemistry I, Faculty of Chemistry and Biochemistry, Ruhr Universität Bochum, D-44780 Bochum, Germany*
[d] *Mahatma Gandhi University Research Centre, Mar Athanasius College, Kothamangalam, 686 666 India*

ABSTRACT

Keywords:
Acetalization
Catalysis
Ce,M–Y zeolites
Diffusional properties
Electron-withdrawing groups
Cation-exchanged montmorillonites

Under ambient reaction conditions, a one-pot acetalization of carbonyl compounds with methanol was carried out over a series of solid acid catalysts. Ion-exchanged montmorillonite samples were prepared by a metal cation (Ce^{3+}, Fe^{3+} and Al^{3+}) exchange from the activated K-10 montmorillonite. These materials have been characterized by wide-angle X-ray scattering (WAXS), solid-state nuclear magnetic resonance spectroscopy (solid-state NMR), temperature programmed desorption of ammonia (NH$_3$-TPD) and Brunauer–Emmett–Teller (BET) analysis. The catalytic results of montmorillonites were compared with those of H–Y, Ce,Na–Y, Ce,H–Y zeolites, SiO$_2$ and γ-Al$_2$O$_3$. Irrespective of the catalyst, the reaction yields the corresponding dimethoxyacetal in high yield. Comparison of the catalytic activity indicates that the montmorillonite catalysts are the most active catalysts for the reaction. The molecular size of the carbonyl substrates is one of the significant factors in determining the acetalization ability of the catalysts, and the activity of ketones follow the order cyclohexanone > 4-nitroacetophenone > acetophenone > 4-methoxybenzophenone > benzophenone. In the aromatic carbonyl compounds, the electron donor or acceptor properties of the substituents are also critical to the reactivity of the acetophenones and benzaldehydes. The aldehydes considered in the present investigation exhibit an activity order of 4-nitrobenzaldehyde > benzaldehyde > 4-methoxybenzaldehyde, which substantiates that electron-withdrawing groups favor the reaction. The reaction time studies indicate that the montmorillonite catalysts are more resistant to deactivation, predominantly due to the superior pore diffusional properties of these materials compared to microporous zeolites.

1. Introduction

Acetals are an important class of compounds that have found direct applications in diverse areas in the chemical industry such as in perfumes, flavours, pharmaceuticals, solvents, and polymer chemistry (Bauer et al., 1990; Clode, 1979; Elliot, 1984; Ley and Priepke, 1994; Sato et al., 1990). The methyl and ethyl acetals of *n*-octanal and *n*-decanal are widely used in the perfume and flavour industries (Arctander, 1969). Several acetals named as 'potential fragrances' are introduced into different formulations so that at the time of contact with the skin, the products are hydrolyzed to release pleasantly odorous compounds. The conversion of a carbonyl compound into its acetal alters its vapor pressure, solubility and aroma characteristics, and can result in flavour attenuation (Burdock, 1995). Moreover,

chiral acetals are particularly important precursors for the preparation of enantiomerically pure compounds (Bartlett et al., 1983). Acetalization is commonly used in protecting group chemistry for carbonyl functional groups because dimethyl acetals and 1,3-dioxolanes are stable under neutral and basic conditions. Their protection as acetals is of paramount importance in organic synthesis, as shown by a large number of methods that have been developed for this key transformation. Various kinds of acids are well known to catalyse the reaction in homogeneous and heterogeneous phases (Banik et al., 2005; Greene and Wuts, 1991; Lin et al., 2001; Lu et al., 1995; Sato et al., 1993). It has been usually performed in the presence of *p*-toluenesulfonic acid, BF$_3$-etherate, FeCl$_3$ or trimethylsilyl trifluoromethanesulfonate (Crimmins and DeLoach, 1986; Dauben et al., 1986; Hwu et al., 1987; Yang et al., 1998).

However, several problems concerning the synthesis of acetals and the protection of carbonyls remain to be solved. The formation of dimethyl acetals in the homogeneous phase is frequently performed by using trimethyl orthoformate as the reagent; however, the use of methanol for the reaction is highly desirable. Many of the acid catalysts

---
* Corresponding author at: University Pierre et Marie Curie, Univ. Paris 06, CNRS, Laboratoire de Chimie de la Matière Condensée de Paris, Collège de France, 11 place Marcellin Berthelot, 75005 Paris, France. Tel.: +91 33 1 44271535; fax: +33 1 44271504.

E-mail address: bejoy.thomas@upmc.fr (B. Thomas).

explored for this transformation present limitations such as extreme reactivity, formation of by-products, toxicity, corrosiveness and tedious work-up procedures (Brown et al., 1964; Climent et al., 2002; Gemal and Luche, 1979). Ever-increasing environmental pressure has pushed the development of environmentally friendly catalysts. In such a context, the production of acetals as carbonyl protecting groups requires the development of new, improved benign procedures, especially based on new selective solid acid catalysts (Cataldo et al., 1999; Climent et al., 1996, 2002; Strukul, 2002; Tanaka et al., 1998).

In recent years, green catalysis has been found to be the method of choice for the production of acetals. For instance, researchers have used many catalysts for the acetalization of carbonyl compounds such as, lanthanum(III)nitrate hexahydrate (Srinivasulu et al., 2008), bismuth subnitrate (Wu et al., 2008), anhydrous $CeCl_3$ (Silveira et al., 2010), cerium(III) trifluoromethanesulfonate (Ono et al., 2009) tetrafluoroboric acid adsorbed on silica gel (Kumar et al., 2008) and phosphotungstic acid and its cesium salt supported on dealuminated ultra-stable Y zeolites (Zhang et al., 2006).

Acidic clays are widely used as catalysts in organic synthesis (Chitnis and Sharma, 1997; Clark and Macquarrie, 1996; Izumi and Onaka, 1992; Nagendrappa, 2011; Sartori et al., 2004) and their acid properties and thus, catalytic performance, depend highly on the exchanged cations. Water molecules in the hydration sphere of the exchanged metal cation can dissociate, producing acidic protons that are potential Brönsted acid sites. These catalysts have many advantages over other catalysts, such as facile modification of acidity via the exchange of cations in the interlayer, ease of handling, non-corrosiveness, low cost and the ability to be regenerated. Moreover, they are environmentally benign. Zhou has recently reviewed the advances in the topic of cation-exchanged montmorillonites (Zhou, 2010). A recent review (Zhang et al., 2010) describes the formation mechanism, physicochemical properties and contemporary applications of various clay minerals.

Solid acid catalysts such as SO_4^{2-}/ZrO_2, SO_4^{2-}/TiO_2 (Lin et al., 2001), acidic zeolites (Algarre et al., 1995; Ballini et al., 1998; Corma et al., 1990; Cejka et al., 2010; Silva et al., 2009), metal cation-exchanged montmorillonites (Kawabata et al., 2001; Tateiwa et al., 1995), mesoporous silica (Iwamoto et al., 2003), and siliceous mesoporous materials (Jermy and Pandurangan, 2006; Rat et al., 2007; Tanaka et al., 1998) have been reported to be active in the acetalization of carbonyls with alcohols. In the present investigation, we report the chemoselective acetalization of ketones and aldehydes with methanol under mild reaction conditions over a series of solid acid catalysts with different pore sizes and acidities.

2. Experimental

2.1. Materials

Pure H–Y and Na–Y zeolites (Si/Al ratio 1.51) were purchased from Sud-Chemie (India) Ltd. K-10 montmorillonite (abbreviated as K-10 mont.), cyclohexanone (99.99%), acetophenone (99.9%), benzophenone (99.9%), 4-methoxyacetophenone (99%), 4-nitroacetophenone (98%), benzaldehyde (99.9%), 4-methoxybenzaldehyde (>99%), and 4-nitrobenzaldehyde (>99%) were acquired from Aldrich Chemical Company, USA and used as received. Analytical grade methanol was procured from SD Fine Chemicals, India and used without further purification. Ammonia (+99.99%) and nitrogen (+99.99%) were purchased from Southern Gas Ltd, India. $Ce(NO_3)_3$ was obtained from Indian Rare Earths Ltd. Udyogamandal, India. $Al(NO_3)_3$ and $Fe(NO_3)_3$ (both ≥98%) were products from Sigma Aldrich, USA. Cerium exchanged M–Y zeolites were obtained by exposing H–Y and Na–Y zeolites to a 0.5 M cerium nitrate solution (0.025 mole of cerium nitrate/g zeolite) at 353 K for 24 h. The samples were calcined after exchange by heating from 423 to 773 K, and then the samples were maintained at 773 K for 5 h with a heating rate of 12 K/min with a constant supply of air (60 mL/min).

2.2. General procedure for the preparation of cation-exchanged montmorillonites

Activated K-10 mont. (>100 mesh, 3 g) was dispersed in 50% aqueous acetone (200 mL) under vigorous magnetic stirring at 298 K for 24 h. The resulting dispersion was heated to 323 K and then added to an aqueous solution (300 mL) of 200 mM of a particular metal salt ($Ce(NO_3)_3$, $Al(NO_3)_3$ and $Fe(NO_3)_3$). The mixture was stirred at 323 K for 24 h. After settling, the resulting wet product was collected by filtration, washed continuously with deionised water and the solid material was collected when cations were no longer detected via qualitative analysis of the filtrate. The solid material was dried at 353 K in an oven for 24 h and then ground and passed through a 100-mesh screen (Tateiwa et al., 1994; Yamanaka and Brindley, 1979).

2.3. Characterization

Catalysts used in the present investigations were characterized by powder X-ray diffraction (Rigaku D-max C X-ray diffractometer with monochromatized Ni-filtered Cu-Kα radiation ($\lambda = 1.5406$ Å) in the radial range of 5–50 degrees), EDAX (JEOL JSM-840 A (Oxford make model l6211 with a resolution of 1.3 eV)), and nitrogen sorption (Micromeritics Gemini surface area analyzer using N_2 as the adsorbate at 77.3 K) studies. For BET analysis the samples were degassed for 3 h at 473 K to remove all the volatiles and chemically adsorbed species from the surface. Nitrogen adsorption data were evaluated as monolayer surface coverage and this protocol gave the specific surface area and the total pore volume of the materials. Results were reproducible within an error limit of 5%.

Wide and small angle X-ray scattering (WAXS and SAXS) measurements of different montmorillonite (abbreviated as mont.) catalysts were performed on a pin-hole type Rigaku Nanoviewer instrument using Cu Kα$_1$ radiation (0.15406 nm) equipped with a CCD detector over a range of 1 to 5° and 1 to 70° respectively under vacuum. The applied voltage and filament current were 40 kV and 50 mA respectively. The finely powdered samples were sealed in metal cells with polyethylene terephthalate films and kept in a temperature controlled sample chamber for measurements. The average acquisition time for the measurements was typically 2–3 h. Bragg spacing was calculated by $d = 2\pi/q$, where q is the magnitude of the scattering vector.

Raman spectroscopy measurements of the Ce-mont. and Fe-mont. catalysts were performed using a modular system (Dilor, LabRAM, ISA Instruments. SA, INC) that consisted of a red He–Ne laser (661 nm) with 60 mW power, a green Ar$^+$ laser (532 nm) with adjustable output power, 100 × 0.9 microscope objective and an Olympus BX40 confocal microscope. The objective used for the Raman spectrometer was 10× and the spectral acquisition time was ca. 120 s. The laser power was set at 60 mW for all measurements.

All NMR experiments of the mont. samples were performed on a Bruker AVANCE III 300 (7.05T) spectrometer. For the {^{1}H}–^{29}Si CP (cross polarization) and {^{1}H}–^{29}Si hpdec (high-power decoupling), MAS NMR studies 7 mm zirconia rotors spinning at 5 kHz were employed. A total of 4200 transients were collected with a proton 90° pulse of 6.5 μs and recycle delays of 1 s for the CP spectra. A cross-polarization contact time of 3 ms was applied for all the experiments. For {^{1}H}–^{29}Si hpdec MAS NMR experiments 1024 transients were collected with a π/4 pulse of 2.65 μs at a relaxation delay of 60 s. The chemical shift values were referenced to tetramethylsilane (TMS) at 0 ppm. ^{27}Al MAS NMR spectra were recorded using a 4 mm triple resonance MAS probe at a spinning frequency of 14 kHz. 4200 transients were collected with a π/12 pulse of 0.95 μs at a repetition

time of 500 ms. The chemical shift was referenced to $Al(NO_3)_3$ at 0 ppm.

The ammonia temperature programmed desorption (NH_3-TPD) of the catalysts was carried out in a stainless steel reactor ($i.d. = 4 \times 5$ mm) packed with about 100 mg catalyst. The catalyst was activated *in situ* at 773 K (473 K for monts.) for *ca.* 1 h in nitrogen flow and allowed to cool to room temperature. It was then poisoned with a stream of NH_3 over 1 h to saturate the surface. Ammonia adsorbed sample was purged with N_2 for *ca.* 2 h at 373 K in order to reduce the extent of physical adsorption on the catalyst surface. NH_3 desorbed while heating from 373 to 873 K was measured quantitatively with a conventional ammonia detector. The amounts of ammonia desorbed were formally divided into three temperature ranges to denote three types of acid sites: (1) weak, 373–473 K, (2) moderate, 473–673 K, and (3) high, 673–873 K.

2.4. Acetalization procedure

Acetalization of the carbonyl compounds was carried out in a 50 mL glass batch reactor equipped with a magnetic stirrer, thermometer, water condenser and temperature controller. All the experiments were performed under dry nitrogen (mass flow controller: Brooks, Model 5896, flow rate: 14 mL/min). In a typical run, 10 mL of a 1:10 molar mixture of ketone and methanol was stirred with 50 mg of catalyst (activated at 773 K (473 K for monts.), 30–40 μm mesh size) for 10 h. Samples were withdrawn every 2 h and at the end of the reaction. Feed and product analysis was performed using gas chromatography (Chemito GC1000). For quantification, a gas chromatograph with a flame ionization detector (FID) was used. For product identification, a gas chromatograph attached to a mass selective detector (Shimadzu-5050 spectrometer) was used. Both the gas chromatographs were equipped with HP-30 methyl siloxane 30 cm × 200 μm × 0.5 μm capillary columns for separation. The temperature program started at 323 K with a hold time of 5 min, followed by a temperature ramp to 403 K at 4 K/min and then to 573 K at 10 K/min. The MS detector voltage was 1 kV. The m/z values and relative percentage intensity were indicated for the significant peaks. A response factor of unity was used for GC-FID product analysis. The % conversion of the carbonyl compounds and the selectivity towards the corresponding acetals were calculated as reported in our previous communications (Thomas and Sugunan, 2004; Thomas et al., 2009).

2.5. Recovery, regeneration and reuse of the catalyst

For a consecutive acetalization, the deactivated catalysts were continuously extracted with dimethyl ether and dried in an oven (383 K for 12 h under air) to remove the remaining surface adsorbed species. The clays were then activated by heating from 423 to 773 K (or 473 K in the case of monts.) over a period of 6 h and maintaining the samples at 773 K for 5 h (dry nitrogen, 60 mL/min). The dry solid was weighed and reused in the subsequent run, maintaining the substrate-to-catalyst and the solvent-to-catalyst ratios constant.

3. Results and discussion

Zeolites in the present investigation were purchased or prepared via cationic exchange. The detailed characterization of the present catalyst systems has already been reported elsewhere (Thomas and Sugunan, 2004, 2005, 2007; Thomas et al., 2005). The physiochemical properties of the catalysts, including, the nSi/nAl ratio, the BET surface area, the pore volume, the number and distribution of the acid strength and the crystallite size (μm) are presented in Table 1. The amounts of Al^{3+}, Ce^{3+} and Fe^{3+} in M^{3+}-monts. were determined by EDAX measurements and the results are depicted in Table 1. Upon cation exchange, the surface area increased and pore volume remained nearly unchanged. The number of acid sites did not vary significantly between the prepared and the as-purchased mont. Variables between all the samples varied greatly, providing a means to examine the relationship between the physicochemical properties and the catalytic performance.

3.1. X-ray scattering studies of mont. catalysts

The WAXS patterns of K-10 mont. and the cation-exchanged counterparts; Ce-mont., Fe-mont. and Al-mont. is shown in Fig. 1. The basal (001) reflection was not very intense in the WAXS pattern, which confirms the partial dealumination of the layered structure of K-10 mont. as reported in the literature (Clark et al., 1994). There is no large shift in the lamellar peak position of the exchanged mont. materials compared to K-10 mont. However, differences in the intensity of the lamellar reflection are observed upon exchange with metal cations. K-10 mont. showed a basal spacing equal to 1.23 nm and the cation-exchanged catalysts exhibited a similar scattering pattern with slightly higher basal spacing. The larger basal spacing of M^{3+}-monts. is due to the displacement of smaller cations such as H^+ and Na^+ in the interlayer space by larger hydrated metal cations. The WAXS patterns of these systems explicitly show the retention of the original clay structure after the cation exchange and thermal conditioning. M^{3+}-monts. calcined at 400 °C showed collapse of the c-axis characteristic of smectites (patterns not shown). The SAXS pattern (see inset of Fig. 1) does not show any reflection in the small angle region (1 to 4°) as expected with smectite clays. The powder

XRD patterns of the monts. are shown in the supplementary information (Fig. S1). For these systems, the characteristic reflections were in the same position, including the two-dimensional hk index pairs 02-11 and 20-13, further indicating the preservation of the two-dimensional lattice after cation exchange and activation. Quartz impurities were significant in all of the systems, and were retained after the cation exchange of the parent K-10 mont. catalyst.

3.2. The oxidation state of exchanged cations in Ce-mont. and Fe-mont

The oxidation state of the exchanged cation is critically important in determining the catalytic activity of metal cation-exchanged monts. Laser Raman spectroscopic studies were performed to evaluate the oxidation state of the exchanged cation in Ce-mont. and Fe-mont. catalysts. CeO_2 has a first order Raman line at 465 cm^{-1} (in nanoparticles at 457 cm^{-1}), which has F_{2g} symmetry and completely dominates the spectra. It has a second order phonon mode at 1174 cm^{-1} (Askrabic et al., 2007; Choi et al., 2006; Weber et al., 1993). The absence of bands at 465 and 1174 cm^{-1} (Fig. 2) confirms the $+3$ oxidation state for cerium in Ce-mont. catalyst. In the case of the Fe-mont., the absence of the strong characteristic bands at *ca.* 292, 411, 692, and 1318 cm^{-1} (Chourpa et al., 2005) implies that iron oxides, such as magnetite (Fe_3O_4) and hematite (Fe_2O_3), are not present in the sample (inset of Fig. 2).

3.3. Solid-state NMR studies of mont. systems

The {^1H}–^{29}Si CP and {^1H}–^{29}Si hpdec MAS NMR spectra of K-10 mont. and the cation-exchanged counterparts respectively are shown in Fig. 3a and b. The ^{29}Si CPMAS NMR spectrum of the original K-10 mont. was composed mainly of two signals. The intense signal located at −101.4 ppm with a full width at half maximum (FWHM) of 6 ppm is due to $[(SiO)_3SiOH]$; a resonance due to silicon bound within amorphous silica with a three-dimensional cross-linked framework. A comparatively less intense signal is centred at −92 ppm with a FWHM of 3 ppm that is due to $Q^2(0Al)$. This signal is attributed to SiO_4 groups in the tetrahedral sheet of mont., which are connected to the zero tetrahedron in which Al for Si substitution occurs (Breen et al., 1995). There were two minor peaks at *ca.* 111 and 87.4 ppm corresponding to $Q^4(4Si0Al)$ and $Q^3(1Al)$ silicon units respectively, which are SiO_4 groups in the tetrahedral (Td) sheet of mont. that are connected to the zero and one Td in which Al for Si substitution occurs respectively. No significant difference was observed in the ^{29}Si CP spectrum upon cation exchange of K-10 mont. with cerium, aluminium and iron.

Komadel et al. (1996) proposed that the −101 signal should be attributed to $Q_4(3Si1Al)$ unit. The strength of this peak increases with contact time (Adams et al., 1991; Tkac et al., 1994), which indicates that the protons in the amorphous SiO_2 prefer the Si-bearing unit corresponding to the −101 signal. Tkac et al. (1994) and Komadel et al. (1996) suggested that in the acid-treated monts. (K-10 mont.) this kind of Si unit could be defined as $(SiO)_3SiOH$, which is identical

to the surface functional groups denoted by Legrand et al. (1993). By using a deconvolution procedure, (see supplementary information, Figs. S2 and S3; also see Table S1 for the ^{29}Si chemical shifts of different silicon units and the corresponding percentages with high-power decoupling and CP MAS NMR spectra) the proportion of the silicon unit corresponding to the −101 ppm peak in different mont. catalysts was not more than 14%, which is different from the values of 20% and 33% reported respectively by Tkac et al. (1994) and Legrand et al. (1993).

^{29}Si CP and hpdec spectra of the samples were extremely different. In the CP MAS NMR spectrum, only three peaks were visible, corresponding to Q_2 (−91.7 ppm), Q_3 (−101.4 ppm), Q_4 (−111.0 ppm). However, the deconvoluted hpdec spectrum showed at least seven peaks, corresponding to the above-mentioned species and to $Si–(O–Al)_n$ species such as Q_3^{nAl} (−85.9 ppm), Q_4^{4Al} (−91.7 ppm), Q_4^{3Al} (−94.4 ppm), Q_4^{2Al} (−101.4 ppm), Q_4^{1Al} (−104.1 ppm) and Q_4^{0Al} (−107.1 ppm). Since these peaks overlap, it is difficult to determine the precise values of the chemical shifts.

As the CP enhances species in proximity with protons, the disappearance of peaks means that these species are unprotonated or are not in close proximity to any protons. On the contrary, even though the Q_4 species are by definition unprotonated, protons are sufficiently close to transfer their polarization. This suggests a phase separation between the silica and the aluminosilicate. Another remarkable difference between the CP and the hpdec is the sideband pattern, which is characteristic from the chemical shift anisotropy (CSA). In the CP spectra the silica species of CSA are almost averaged at a spinning frequency of 5 kHz, as is common in amorphous silica. On the contrary, in the hpdec spectra, the residual CSA is not at all negligible, suggesting an ordered phase in the aluminosilicate, which is in agreement with the mont. structure.

The most prominent structural effect on the isotropic ^{27}Al chemical shifts of aluminosilicates is the coordination number of AlO_n polyhedra. ^{27}Al MAS NMR provides information about the environment of the aluminium ions in mont. and the cation-exchanged equivalents (Fig. 4). For K-10 mont., two asymmetric lines of the aluminium nuclei were observed. The major line at *ca.* 0 ppm is related to the octahedral coordination of the aluminium ions, whereas the line at *ca.* 60 ppm indicates that some of the ^{27}Al ions are present in a tetrahedral environment (Engelhardt and Michel, 1987; Molis et al., 2001; Salerno and Mendioroz, 2002). These coordination states appear as a consequence of isomorphic ion substitution within the layers of the clay structure. However, the tetrahedral aluminium component was more complex, presumably due to the presence of more than one Al^{IV} site. The spectra showed shoulders at 51 and 54 ppm in addition to the main resonances at 65 ppm. The distribution of chemical shifts of the tetrahedral aluminium suggests a somewhat different local structure in the original layered structure. Comparable peak distribution was observed in M^{n+}-mont., and a rather similar distribution of chemical shifts has been reported by Okada et al. (2006) in various acid-activated clays. This chemical shift distribution was more clearly seen in the case of the parent K-10 mont., however, it was not very predominant in the case of Fe-mont. This could be explained as an effect of the paramagnetic Fe species on the relaxation of the aluminium nuclei. After the clay structure modification by cation exchange, there was no significant intensity variation for either the tetrahedral or the octahedral line, further demonstrating the preservation of the clay structure upon cation exchange and activation.

3.4. Acetalization of aldehydes and ketones

Acetal formation is reversible and the reaction has two parts; an alcohol reacts with the carbonyl group to produce hemiacetals. These further react with another alcohol molecule to form an acetal. The reaction rate and degree of reaction are strongly affected by electronic

and steric factors. A detailed acetalization mechanism over solid acid catalysts is depicted in the supplementary information (Scheme S1).

The reaction proceeds via the formation of bulky intermediates and consequently microporous materials like zeolites are apparently less effective compared to mesoporous mont. catalysts. From this point of view, we have investigated the catalytic efficiency of a series of solid acid catalysts with different pore characteristics such as monts., zeolites and some common oxide catalysts towards acetalization of ketones such as cyclohexanone, acetophenone, benzophenone, 4-methoxyacetophenone and 4-nitroacetophenone (Table 2), and aldehydes; benzaldehyde, 4-methoxybenzaldehyde and 4-nitrobenzaldehyde (Table 3). In all cases, only the corresponding acetal was obtained in the reaction mixture after 10 h of reaction time.

In the present investigation, K-10 and cation-exchanged monts. were found to be the most active catalyst for the substrate-selective acetalization of ketones and aldehydes. The cation-exchanged monts. were more active compared to the parent K-10 mont. Ce-mont. was found to be the most effective catalyst for the reaction, while Ce,H–Y is the most active among zeolites. Silica and γ-alumina exhibit negligible activity owing to their pore structure and the reduced acid strength. There was a considerable increase in the percentage conversion with reaction time. Among different ketones, cyclohexanone showed the maximum conversion (cyclohexanone is more reactive towards nucleophiles), whereas benzophenone the least. Ce-mont. showed a conversion of 78.9, 21.2, 4.1, 28.4 and 19.1% with cyclohexanone, acetophenone, benzophenone, 4-nitroacetophenone and 4-methoxyacetophenone, whereas over Ce,H–Y it was 70.1, 12.5, 2.5, 14.8 and 10.2% respectively. The acetalization of aromatic ketones in general had decreased activity, which might be due to the resonance effect. This is because aromaticity leads to a special stability in the reactant that causes net deactivation towards nucleophilic attack. The synthesis of dialkyl acetals from diaryl ketones is more difficult, and the standard acetalization conditions generally do not work with diaryl ketones. Indirect routes have been developed for their preparation (Leonard et al., 2002a,b). No conversion was observed in a blank run.

The difference in the catalytic activity of zeolites, monts. and oxide catalysts towards the acetalization reaction was studied in detail. Results of acidity measurements illustrate that zeolites were far more acidic than monts. or oxide catalysts. In terms of acid structural properties, zeolites must be more active than mont. catalysts. According to TPD studies, the Ce,Na–Y zeolite was the most acidic and had the highest number of acid sites (2.24 mmol/g) among the catalysts, however, it produced less of the acetal compared to monts. and Ce,H–Y zeolite (2.02 mmol/g). The greater activity of Ce,H–Y zeolite compared to Ce,Na–Y zeolite is due to the specific influence of H^+ due to its high polarizing nature and small size compared to sodium, which affects the –OH bond throughout the zeolite lattice (Brönsted acidity). For a given carbonyl compound, the presence of these –OH groups help in pushing the equilibrium reaction towards acetal formation.

The active sites involved in the reaction were thought to be bridging hydroxyl groups, which must be related to the presence of tetrahedrally coordinated aluminiums in the structure. Bridging hydroxyl groups are present in much larger quantities in zeolites and must have a higher intrinsic activity than monts., which have weaker acid sites related to presence of silanol groups (Climent et al.,

1996). However monts. produce a higher degree of acetalization. Accordingly, it is not just the acid properties of the catalysts, but the pore sizes of these materials that have a predominant influence on acetalization. This might be due to the higher surface accessibility in materials with larger pore sizes (Drisko et al., 2009). Over the zeolites and the other catalysts used in the present investigation, pore diffusion limitations imposed by large molecular sizes (0.75, 1.03, 1.13, 1.19, and 1.20 nm respectively for cyclohexanone, acetophenone, 4-nitroacetophenone, benzophenone and 4-methoxyacetophenone; as determined by the energy minimization program) of the ketones played an important role in the acetalization. Corma et al. (1990) have illustrated a similar point earlier. Catalytic activity towards the acetalization reaction does not require strongly acidic sites, and investigations revealed that a regular mesostructure and the size of the pores of the catalysts were important to obtain high activity (Climent et al., 1996; Iwamoto et al., 2003; Jermy and Pandurangan, 2006; Rat et al., 2007). However, the larger conversion of 4-nitroacetophenone than acetophenone and 4-methoxyacetophenone highlights the significance of the substituents' electronic effects on the acetalization over solid acid catalysts.

The acid strength, the pore sizes of the catalyst systems and the electronic effects of the carbonyl compounds are not the only deciding factors in the acetalization reaction. The pore structure of the catalyst is also critically important. The zeolite-Y has a 3-D interconnected pore

system with super cages of 1.18 nm connected by circular 12-ring 0.74 nm windows (Baur, 1964). Mont. is a three-layer aluminosilicate clay composed of a central alumina sheet sandwiched between two tetrahedral silica sheets. The average pore size (>1.0 nm) was more than in zeolites (Atkins et al., 1983; Edelman and Favejee, 1940). A fraction of the acid sites on the outer surface of the zeolites were available for reactants and therefore higher product yield could only be achieved by performing the reaction for longer times (Tables 2 and 3). Monts. have mesopores and the faster diffusion rates in these materials than in the microporous zeolites increased the catalytic rate.

Acetalization of 4-substituted benzaldehydes and acetophenones having either electron-donating or electron-withdrawing groups employs electrostatic interactions. The 4-substituted aromatic carbonyl compounds undergo acetalization and results in varying yields. As reported in the literature (Gopinath et al., 2002; Jermy and Pandurangan, 2005; Leonard et al., 2002a,b), aromatic aldehydes and ketones with stronger electron-donor groups, such as methoxy groups, have increased electron density on the carbonyl carbon making it less susceptible to nucleophilic attack by methanol. Thus, moieties with an electron donor in the ortho- or para-position showed less reactivity and gave lower yields. Conversely, an electron-withdrawing group, such as nitro, lowers electron density on the carbonyl carbon and therefore increases the susceptibility to nucleophilic attack by methanol. Hence, the electron-withdrawing groups promote the acetalization reaction and on the other hand electron-donating groups do not favour the reaction. The order of reactivity of aromatic aldehydes and para-substituted acetophenones in the present investigation is completely in agreement with earlier reports regarding the influence of electronic effects on acetalization.

Cerium exchanged catalysts; Ce,M–Y zeolites and Ce-mont. catalysts produced larger quantities of acetals compared to H–Y zeolite, K-10 mont. or other M^{n+}-monts. Tateiwa et al. (1995) reported the acetalization of carbonyl compounds with methanol in the presence of different cation-exchanged monts. (M^{n+}-mont.; $M^{n+} = Ce^{3+}$, Zr^{4+}, Fe^{3+}, Al^{3+}, Zn^{2+}, H^+, and Na^+). They proposed that in the case of Ce-mont. the carbonyl oxygen presumably coordinates to the Ce^{3+} cation in the interlayer space as well as to an aluminium atom, a potential Lewis acid site, in the framework clay facilitating the active adsorption of ketones (Higuchi et al., 1993; Tateiwa et al., 1995). Furthermore, a Ce^{3+} cation can in principle act as a Lewis acid site and thus can activate the carbonyl group by coordination, in the order of 1 kJ mol^{-1} (Tateiwa et al., 1995). The high activity of K-10 and M^{n+}-monts. were comparable to those of sulphonic acid resins (Olah et al., 1981; Patwardhan and Dev, 1974). UV–vis DRS (ultraviolet–visible-diffuse reflectance spectroscopy) studies on Ce,M–Y zeolites and Ce-mont. catalysts (an intense band around 300 nm due to $Ce^{3+} \leftrightarrow Ce^{4+}$ charge transfer, not shown), confirmed the presence of only one type of well dispersed cerium species in the tetra-coordinate state (Che and Verduraz, 1999; Laha et al., 2002). Greater dispersion of tetra-coordinated cerium in Ce,M–Y zeolites and Ce-mont. catalysts throughout the porous silicate framework could be corroborated to the enhanced acetalization activity of these catalysts compared to other solid acid catalysts. In the case of cyanosilation and Mukaiyama aldol reactions, the carbonyl group was activated by a strong Brönsted acid site induced by exchangeable cations (Fe^{3+} and Al^{3+}) in the interlayer space of the clay material, and similar carbonyl group activation is expected in M^{n+}-monts., which explains their enhanced catalytic activity.

3.5. The effect of the reaction time

Acetalization of cyclohexanone and 4-nitrobenzaldehyde was performed over H–Y, Ce,H–Y zeolites and Ce-mont. for 50 h. Results of the time on stream studies of these catalysts are shown in Fig. 5 and supplementary information (Fig. S4). The reaction reached equilibrium in ca. 60 minutes and the yield of 1,1-dimethoxycyclohexane was 68.7% with Ce,H–Y zeolite. Once the reaction attained equilibrium

there was only a small increase in the production of acetal over Ce, H–Y zeolite (80.5% in 50 h). Furthermore, Ce-mont., while having slightly higher initial activity (73.8% in 1 h), can eventually achieve a larger conversion (100% in 50 h). This variation is due to the major difference in the nature of deactivation of these catalysts. The bulky reaction products and intermediates formed can adsorb in the 3D cavities of zeolite-Y catalysts, thereby blocking the pores and/or active sites and leading to a loss of catalytic activity. Adsorption and the resultant pore filling in the larger pores of the Ce-mont. catalyst (>1.0 nm) is to a limited extent and consequently, diffusion is less hindered and the yield of 1,1-dimethoxycyclohexane and 1,1-dimethoxy-4-nitrobenzene increases with reaction time. In conclu-sion, catalyst deactivation studies indicated that while zeolites and monts. have slightly different initial activity, zeolites deactivate much more rapidly owing to the pore blocking lower diffusion rates of the bulky reaction intermediates and products within the microporous structure. Another reason for the decrease in activity over time could be that the residual water produced during the reaction was poisoning the catalyst.

Deactivated catalysts have been regenerated by solvent extraction to remove products adsorbed onto the active sites. Thus, spent catalysts (H–Y, Ce,H–Y zeolites and Ce-mont.) were subjected to solid–liquid extraction with dichloromethane several times. The as-extracted catalysts showed less than 50% activity towards the acetalization of cyclohexanone. These samples were then reactivated at 773 K (473 K for Ce-mont. catalyst) for 5 h under a constant flow of dry nitrogen (60 mL/h). A third use of the catalyst exhibited no substantial loss of activity or change in the product distribution (Table 4). Furthermore, ^{27}Al MAS NMR spectra of the regenerated zeolites and mont. catalyst showed no considerable increase in the amount of extra-framework aluminium compared to those before exposure to the organic substrate. This observation demonstrates that the catalysts can be regenerated without damage to the framework or loss of catalytic activity. However, a comparison of the percentage activity loss between the first and the third cycle among Ce,H–Y zeolite and Ce-mont. catalysts (1.4 and 3.4% respectively during acetalization of 4-nitrobenzaldehyde) were observed. This greater stability of Ce,H–Y zeolite towards reuse could be due to the stronger zeolite framework, which prevents even minor dealumination and subsequent loss of catalytic activity during catalytic reaction and regenerative heat treatment compared to the monts.

We have conducted additional experiments to obtain comprehensive evidence for the true heterogeneity of these catalytic reactions. Acetalization of cyclohexanone was performed using a Ce,H–Y zeolite and Ce, Fe and Al exchanged monts. under standard reaction conditions for 10 h and the products were separated by filtration. The presence of Al^{3+}, Ce^{3+} or Fe^{3+} was not detected in the product by energy dispersive X-ray (JEOL JSM-840A; Oxford model 16211) analysis or by qualitative chemical analysis of the product mixture. These results strongly suggest that leaching of Ce^{3+}, Al^{3+} or Fe^{3+} cation from the catalysts during the reaction is not occurring.

4. Conclusions

A series of solid acid catalysts was used for the one-pot acetalization of carbonyl compounds with methanol under ambient reaction conditions and the corresponding dimethylacetal was obtained in high yield. Formation of hemiacetal was not observed with any of the catalysts. K-10 mont. and the cation-exchanged counterparts exhibit superior catalytic efficiency than the more highly acidic zeolites. Ce-mont. was the most effective for the substrate-selective acetalization of aldehydes and ketones. The enhanced acetalization activity of Ce exchanged materials compared to other monts. and zeolite can be attributed to the excellent dispersion of tetra-coordinated cerium in Ce-mont. and Ce,M−Y zeolites throughout the porous silicate framework. The molecular size and electronic properties of the carbonyl compounds, and the pore size of the solid acid catalysts were critical factors influencing the acetalization activity. The activity of ketones follows the order cyclohexanone > 4-nitroacetophenone > acetophenone > 4-methoxy acetophenone > benzophenone, which is in the reverse order of molecular size. Aldehydes considered in the present investigation exhibited an activity order of 4-nitrobenzaldehyde > benzaldehyde > 4-methoxybenzaldehyde. Time on stream studies illustrated that the catalyst decay is greater over zeolites than over the monts. The present findings demonstrate the potentials of these materials as solid acid catalysts for acetalization for an environmentally benign approach.

Acknowledgements

Appendix A. Supplementary data

Supplementary data to this article can be found online at doi:10.1016/j.clay.2011.01.021.

References

Adams, S.J., Hawkes, G.E., Curzon, E.H., 1991. A solid-state ^{29}Si nuclear magnetic resonance study of opal and other hydrous silica. Am. Mineralog. 76, 1863.

Algarre, F., Corma, A., Garcia, H., Primo, J., 1995. Acid zeolites as catalysts in organic reactions: highly selective condensation of 2-alkylfurans with carbonylic compounds. Appl. Catal. A. Gen. 128, 119–126.

Arctander, S., 1969. Perfumery and Flavour Chemicals. Vols. I. II. Allured Publishing, New York.

Askrabic, S., Kostic, R., Dohcevic-Mitrovic, Z., Popovic, Z.V., 2007. Raman scattering from low frequency phonons confined in CeO₂ nanoparticles. J. Phys. Conf. Ser 92, 1–4.

Atkins, M.P., Smith, D.J.H., Westlake, D.J., 1983. Montmorillonite catalysts for ethylene hydration. Clay Miner. 18, 423–429.

Ballini, R., Bosica, G., Frullanti, B., Maggi, R., Sartori, G., Schroer, F., 1998. 1,3-Dioxolanes from carbonyl compounds over zeolite HSZ-360 as a reusable, heterogeneous catalyst. Tetrahedron Lett. 39, 1615–1618.

Banik, B.K., Chapa, M., Marquez, J., Cardona, A., 2005. A remarkable iondine-catalyzed protection of carbonyl compounds. Tetrahedron Lett. 46, 2341–2343.

Bartlett, P.A., Johnson, W.S., Elliott, J.D., 1983. Asymmetric synthesis via acetal templates. 3. on the stereochemistry observed in the cyclization of chiral acetals of polyolefinic aldehydes; formation of optically active homoallylic alcohols. J. Am. Chem. Soc. 105, 2088–2089.

Bauer, K., Garbe, D., Surburg, H., 1990. Common Fragrances and Flavour Materials, 2nd edition. VCH, New York.

Baur, W.H., 1964. On the cation and water positions in faujasite. Am. Mineralog. 49, 697–704.

Breen, C., Madejova, J., Komadel, P., 1995. Correlation of catalytic activity with infra-red, ^{29}Si MAS NMR and acidity data for HCl-treated fine fractions of montmorillonites. Appl. Clay Sci. 10, 219–230.

Brown, J.J., Lenhard, R.H., Bernstein, S., 1964. Steroidal cyclic ketals. XXV.[1] the preparation of steroidal δ⁴-3-ethyleneketals. J. Am. Chem. Soc. 86, 2183–2187.

Burdock, G.A., 1995. Fenaroli's Handbook of Flavour Ingredients, Vol. 2. CRC, New York.

Cataldo, M., Neiddu, F., Gavagnin, R., Pinna, F., Strukul, G., 1999. Hydroxy complexes of palladium (II) and platinum (II) as catalysts for acetalization of aldehydes and ketones. J. Mol. Catal. Chem. 142, 305–316.

Cejka, J., Corma, A., Zones, S., 2010. Zeolites and Catalysis: Synthesis, Reactions and Applications. Wiley-VCH Verlag GmbH & Co, Weinheim.

Che, M., Verduraz, F.B., 1999. UV–Vis- and EPR Spectroscopies. In: Ertl, G., Knozinger, H., Weitkamp, J. (Eds.), Handbook of Heterogeneous Catalysis, vol. 2. VCH, Wiley, p. 640.

Chitnis, S.R., Sharma, M.M., 1997. Industrial applications of acid-treated clays as catalysts. React. Funct. Polym. 32, 93–115.

Choi, Y.M., Abernathy, H., Chen, H.-T., Lin, M.C., Liu, M., 2006. Characterization of O₂–CeO₂ interactions using in situ Raman spectroscopy and first first principle calculation. Chem. Phys. Chem. 7, 1957–1963.

Chourpa, I., Douziech-Eyrolles, L., Ngaboni-Okassa, L., Fouquenet, J.-F., Cohen-Jonathan, S., Souce, M., Marchais, H., Dubois, P., 2005. Molecular composition of iron oxide nanoparticles, precursors for magnetic drug targeting, as characterized by confocal Raman microspectroscopy. Analyst 130, 1395–1403.

Clark, J.H., Macquarrie, D.J., 1996. Environmentally friendly catalytic methods. Chem. Soc. Rev. 25, 303–310.

Clark, J.H., Cullen, S.R., Barlow, S.J., Bastock, T.W., 1994. Environmentally friendly chemistry using supported reagent catalysts: structure–property relationships for clayzic. J. Chem. Soc. Perkin Trans. 2, 1117–1130.

Climent, M.J., Corma, A., Iborra, S., Navarro, M.C., Primo, J., 1996. Use of mesoporous MCM-41 aluminosilicate as catalysts in the production of fine chemicals: preparation of dimethylacetals. J. Catal. 163, 783–789.

Climent, M.J., Velty, A., Corma, A., 2002. Design of a solid catalyst for the synthesis of a molecule with blossom orange scent. Green Chem. 4, 565–569.

Clode, D.M., 1979. Carbohydrate cyclic acetal formation and migration. Chem. Rev. 79, 491–513.

Corma, A., Climent, M.J., Garcia, H., Primo, J., 1990. Formation and hydrolysis of acetals catalysed by acid faujasites. Appl. Catal. 59, 333–340.

Crimmins, M.T., DeLoach, J.A., 1986. Intramolecular photocycloadditions-cyclobutane fragmentation: total synthesis of (.+-.)-pentalenene, (.+-.)-pentalenic acid, and (.+-.)-deoxypentalenic acid. J. Am. Chem. Soc. 108, 800–806.

Dauben, W.G., Gerdes, J.M., Look, G.C., 1986. Organic reactions at high pressure. Conversion of cyclic alkanones and enones to 1, 3-dioxolanes. J. Org. Chem. 51, 4964–4970.

Drisko, G.L., Luca, V., Sizgek, E., Scales, N., Caruso, R.A., 2009. Template synthesis and adsorption properties of hierarchically porous zirconium titanium oxides. Langmuir 25, 5286–5293.

Edelman, C.H., Favejee, J.C.L., 1940. On the crystal structure of montmorillonite and halloysite. Z. Kristallogr. Al02, 417–431.

Elliot, A.J., 1984. 1, 3-Dioxalane Polymers in Comprehensive Heterocyclic Polymers, vol. 6. Pergamon Press, Oxford, UK.

Engelhardt, G., Michel, D., 1987. High-resolution Solid-state NMR of Silicates and Zeolites. Wiley, New York, USA.

Gemal, A.L., Luche, J.-L., 1979. Lanthanoids in organic synthesis. 4. selective ketalization and reduction of carbonyl groups. J. Org. Chem. 44, 4187–4189.

Gopinath, R., Haque, Sk.J., Patel, B.K., 2002. Tetrabutylammonium tribromide (TBATB) as an efficient generator of HBr for an efficient chemoselective reagent for acetalization of carbonyl compounds. J. Org. Chem. 67, 5842–5845.

Greene, T.W., Wuts, P.G.M., 1991. Protective Groups in Organic Synthesis, 2nd edition. John Wiley & Sons, Inc., New York, pp. 178–180.

Higuchi, K., Onaka, M., Izumi, Y., 1993. Solid acid and base-catalyzed cyanosilylation of carbonyl compounds with cyanotrimethylsilane. Bull. Chem. Soc. Jpn 66, 2016–2032.

Hwu, J.R., Leu, L.-C., Robl, J.A., Anderson, D.A., Wetzel, J.M., 1987. General scope of 1, 3-dioxolanation of alpha., beta.-unsaturated aldehydes with 1, 2-bis(trimethylsilyloxy)ethane and trimethylsilyl trifluoromethanesulfonate. J. Org. Chem. 52, 188–191.

Iwamoto, M., Tanaka, Y., Sawamura, N., Namba, S., 2003. Remarkable effect of pore size on the catalytic activity of mesoporous silica for the acetalization of cyclohexanone with methanol. J. Am. Chem. Soc. 125, 13032–13033.

Izumi, Y., Onaka, M., 1992. Organic syntheses using aluminosilicates. Adv. Catal. 38, 245–282.

Jermy, B.R., Pandurangan, A., 2005. H₃PW₁₂O₄₀ supported on MCM-41 molecular sieves: an effective catalyst for acetal formation. Appl. Catal A: Gen 295, 185–192.

Jermy, B.R., Pandurangan, A., 2006. A1-MCM-41 as an efficient heterogeneous catalyst in the acetalization of cyclohexanone with methanol, ethylene glycol and pentaerythritol. J. Mol. Catal. A. Chem. 256 (1–2), 184–192.

Kawabata, T., Mizugaki, T., Ebitani, K., Kaneda, K., 2001. Highly efficient heterogeneous acetalization of carbonyl compounds catalyzed by a titanium cation-exchanged montmorillonite. Tetrahedron Lett. 42, 8329–8332.

Komadel, P., Madejova, J., Janek, M., 1996. Dissolution of hectorite in inorganic acids. Clays Clay Miner. 44 (2), 228–236.

Kumar, D., Kumar, R., Chakraborti, A.K., 2008. Tetrafluoroboric acid adsorbed on silica gel as a reusable heterogeneous dual-purpose catalyst for conversion of aldehydes/ketones into acetals/ketals and back again. Synthesis 1249–1256.

Laha, S.C., Mukherjee, P., Sarkar, S.R., Kumar, R., 2002. Cerium containing MCM-41-type mesoporous materials and their acidic and redox catalytic properties. J. Catal. 207, 213–223.

Legrand, A.P., Taibi, H., Hommel, H., 1993. Silicon functionality distribution on the surface of amorphous silica by ^{29}Si solid state NMR. J. Non-Cryst. Solids 155, 122–130.

Leonard, N.M., Oswald, M.C., Freiberg, D.A., Nattier, B.A., Smith, R.C., Mohan, R.S., 2002a. A simple and versatile method for the synthesis of acetals from aldehydes and ketones using bismuth triflate. J. Org. Chem. 67, 5202–5207.

Leonard, N.M., Weiland, L.C., Mohan, R.S., 2002b. Applications of bismuth(III) compounds in organic synthesis. Tetrahedron 58, 8373–8397.

Ley, S.V., Priepke, H.W.M., 1994. A facile one-pot synthesis of a trisaccharide unit from the common polysaccharide antigen of group b *streptococci* using cyclohexane-1,2-diacetal (cda) protected rhamnosides. Angew. Chem. Int. Ed Engl. 33, 2292–2294.

Lin, C.-H., Lin, S.D., Yang, Y.-H., Lin, T.-P., 2001. The synthesis and hydrolysis of dimethyl acetals catalyzed by sulfated metal oxides. An efficient method for protecting carbonyl groups. Catal. Lett. 73, 121–125.

Lu, T.-J., Yang, J.-F., Sheu, L.-J., 1995. An efficient method for the acetalization of α,β-unsaturated aldehydes. J. Org. Chem. 60, 2931–2934.

Molis, E., Thomas, F., Faisandier, K., Bihannic, I., 2001. Structural collapse of Al$_{13}$-intercalated montmorillonite by Na-salicylate solutions. Clay Miner. 36, 335–344.

Nagendrappa, G., 2011. Organic synthesis using clay and clay-supported catalysts. Appl. Clay Sci. doi:10.1016/j.clay.2010.09.016. Article in press.

Okada, K., Arimitsu, N., Kameshima, Y., Nakajima, A., MacKenzie, K.J.D., 2006. Solid acidity of 2:1 type clay minerals activated by selective leaching. Appl. Clay Sci. 31, 185–193.

Olah, G.A., Narang, S.C., Meidar, D., Salem, G.F., 1981. Catalysis by solid superacids; 8^1. improved nafion-H^2 perfluorinated resinsulfonic acid-catalyzed preparation of dimethyl acetals and ethylenedithioacetals, and hydrolysis of dimethyl acetals. Synthesis 282–283.

Ono, F., Inatomi, Y., Tada, Y., Mori, M., Sato, T., 2009. A facile procedure for acetalization of aldehydes and ketones catalyzed by cerium(III) trifluoromethanesulfonate. Chem. Lett. 38, 96.

Patwardhan, S.A., Dev, S.U.K.H., 1974. Amberlyst-15, a superior catalyst for the preparation of enol ethers and acetals. Synthesis 348–349.

Rat, M., Zahedi-Niaki, M.H., Kaliaguine, S., Trong-On, Do, 2007. Synthesis and catalytic properties of sulfonic acid-functionalized periodic mesoporous organosilicas. Stud. Surf. Sci. Catal. 170B, 1811–1818.

Salerno, P., Mendioroz, S., 2002. Preparation of Al-pillared montmorillonite from concentrated dispersions. Appl. Clay Sci. 22 (3), 115–123.

Sartori, G., Ballini, R., Bigi, F., Bosica, G., Maggi, R., Righi, P., 2004. Protection (and deprotection) of functional groups in organic synthesis by heterogeneous catalysis. Chem. Rev. 104, 199–250.

Sato, T., Otera, J., Nozaki, H., 1990. Organotin triflate promoted carbonyl activation. Does acetalization deactivate or activate carbonyl groups? J. Am. Chem. Soc. 112, 901–902.

Sato, T., Otera, J., Nozaki, H., 1993. Differentiation between carbonyls and acetals in 1,3-dithiane and 1,3-dithiolane synthesis catalyzed by organotin triflates. J. Org. Chem. 58, 4971–4978.

Silva, da C.X.A., Goncalves, V.L.C., Mota, C.J.A., 2009. Water-tolerant zeolite catalyst for the acetalisation of glycerol. Green Chem. 11, 38–41.

Silveira, C.C., Mendes, S.R., Ziembowicz, F.I., Lenardão, E.J., Perin, G., 2010. The use of anhydrous CeCl$_3$ as a recyclable and selective catalyst for the acetalization of

aldehydes and ketones. J. Braz. Chem. Soc. 21, 371–374.

Srinivasulu, M., Suryakiran, N., Rajesh, K., Reddy, S.M., Venkateswarlu, Y., 2008. Mild and efficient chemoselective synthesis of acetals and geminal diacetates (acylals) from aldehydes using lanthanum (iii) nitrate hexahydrate. Synth. Commun. 38, 1753–1759.

Strukul, G., 2002. Lewis acid behaviour of cationic complexes of palladium (II) and platinum (II): some examples of catalytic applications. Top. Catal. 19, 33–42.

Tanaka, Y., Sawamura, N., Iwamoto, M., 1998. Highly effective acetalization of aldehydes and ketones with methanol on siliceous mesoporous materials. Tetrahedron Lett. 39, 9457–9460.

Tateiwa, J., Horiuchi, H., Hashimoto, K., Yamauchi, T., Uemura, S., 1994. Cation-exchanged montmorillonite-catalyzed facile Friedel–Crafts alkylation of hydroxy and methoxy aromatics with 4-hydroxybutan-2-one to produce raspberry ketone and some pharmaceutically active compounds. J. Org. Chem. 59, 5901–5904.

Tateiwa, J., Horiuchi, H., Uemura, S., 1995. Ce^{3+}-exchanged montmorillonite (Ce^{3+}-mont) as a useful substrate-selective acetalization catalyst. J. Org. Chem. 60, 4039–4043.

Thomas, B., Sugunan, S., 2004. Influence of residual cations (H$^+$, Na$^+$, K$^+$, and Mg^{2+}) in the alkylation activity of benzene with 1-octene over rare earth metal ion exchanged FAU-Y zeolite. Microporous Mesoporous Mater. 72, 227–238.

Thomas, B., Sugunan, S., 2005. Alkylation of benzene with 1-octene over rare earth exchanged HFAU-Y zeolites. React. Kinet. Catal. Lett. 85, 29–36.

Thomas, B., Sugunan, S., 2007. Dehydration of aldoximes on rare earth exchanged (La^{3+}, Ce^{3+}, RE^{3+}, Sm^{3+}) Na–Y zeolites: a facile route for the synthesis of nitriles. J. Porous Mater. 14, 471–480.

Thomas, B., Prathapan, S., Sugunan, S., 2005. Solid acid-catalyzed dehydration/Beckmann rearrangement of aldoximes: towards high atom efficiency green processes. Microporous Mesoporous Mater. 79, 21–27.

Thomas, B., George, J., Sugunan, S., 2009. Synthesis of benzoxazole via the Beckmann rearrangement of salicylaldoxime on protonated zeolites: a green continuous process. Ind. Eng. Chem. Res. 48, 660–670.

Tkac, I., Komadel, P., Müller, D., 1994. Acid-treated montmorillonites—a study by ^{29}Si and ^{27}Al MAS NMR. Clay Miner. 29, 11–19.

Weber, W.H., Hass, K.C., McBridge, J.R., 1993. Raman study of CeO$_2$: second-order scattering, lattice dynamics, and particle effects. Phys. Rev. B 48, 178–185.

Wu, S., Dai, W., Yin, S., Li, W., Au, C.-T., 2008. Bismuth subnitrate as an efficient heterogeneous catalyst for acetalization and ketalization of carbonyl compounds with diols. Catal. Lett. 124, 127–132.

Yamanaka, S., Brindley, G.W., 1979. High surface area solids obtained by reaction of montmorillonite with zirconyl chloride. Clays Clay Miner. 27, 119–124.

Yang, H., Li, B., Cui, Y., 1998. Preparation of salicylic acid resin supported FeCl$_3$ Lewis acid catalyst and its application in organic synthesis. Synth. Commun. 28, 1233–1238.

Zhang, F., Yuan, C., Wang, J., Kong, Y., Zhu, H., Wang, C., 2006. Synthesis of fructone over dealuminated USY supported heteropoly acid and its salt catalysts. J. Mol. Catal. Chem. 247, 130–137.

Zhang, D., Zhou, C.H., Lin, C.-X., Tong, D.-S., Yu, W.-H., 2010. Synthesis of clay minerals. Appl. Clay Sci. 50, 1–11.

Zhou, C.-H., 2010. Emerging trends and challenges in synthetic clay-based materials and layered double hydroxides. Appl. Clay Sci. 48, 1–4.

Table 1

General feature of the zeolites, montmorillonites, SiO$_2$, and γ-Al$_2$O$_3$ used in the acetalization of carbonyl compounds with methanol.

Catalyst	Si/Al[a]	Amount of exchanged cation (%)	S$_{BET}$ (m^2 g^{-1})	Pore volume[c] (cm^3 g^{-1})	Amount of ammonia (mmol/g)[d]				Crystallite size (μm)[g]
					W[e,f]	M[e]	S[e]	Cumulative	
H–Y	1.51	–	398	0.266	0.69	0.41	0.33	1.43	0.90
Ce,H–Y	1.51	–	511	0.340	1.10	0.60	0.31	2.02	0.93
Ce,Na–Y	1.51	–	484	0.296	1.45	0.59	0.20	2.24	0.95
K-10 mont.	2.70[b]	–	183	0.204	0.55	0.24	0.13	0.92	≈1.0
Ce^{3+}-mont.	2.70[b]	1.97[b]	221	0.207	0.56	0.28	0.18	1.02	≈1.0
Al^{3+}-mont.	2.44[b]	2.10[b]	208	0.201	0.53	0.26	0.20	0.99	≈1.0
Fe^{3+}-mont.	2.70[b]	2.34[b]	198	0.199	0.53	0.23	0.19	0.95	≈1.0
SiO$_2$	–	–	155	0.172	0.59	0.11	0.07	0.77	≈1.11
γ-Al$_2$O$_3$	–	–	162	0.181	0.56	0.19	0.13	0.88	≈1.04

[a] As determined by Inductively Coupled Plasma-Atomic Emission Spectroscopy (ICP-AES; Perkin Elmer) analysis.
[b] As determined by energy dispersive X-ray analysis.
[c] Total pore volume measured at 0.9976 P/P$_0$.
[d] As determined by temperature programmed desorption of ammonia in the temperature range 373–873 K.
[e] W, M, and S stand for weak (373–473 K), medium (474–673 K), and strong (674–873 K) acid sites.
[f] Ammonia desorbed in the 373–473 K temperature range might also contain some physisorbed ammonia.
[g] As determined by powder X-ray diffraction studies.

Table 2
Results obtained from the acetalization of cyclohexanone, acetophenone, 4-nitroacetophenone, 4-methoxyacetophenone and benzophenone, with methanol over different solid acid catalysts.

Catalyst	Percentage conversion of ketones									
	Cyclohexanone		Acetophenone		Benzophenone		4-Nitro-acetophenone		4-Methoxy-benzophenone	
	2 h	10 h	2 h	10 h	2 h	10 h	2 h	10 h	2 h	10 h
H–Y	43.6	49.9	4.4	7.6	1.2	2.4	4.9	7.2	2.9	7.2
Ce,H–Y	70.1	79.7	12.5	20.1	2.5	5.2	14.8	25.0	10.2	17.8
Ce,Na–Y	64.2	71.5	7.9	13.1	1.9	4.1	10.1	17.3	6.8	11.6
K-10 mont.	71.7	88.2	13.8	21.2	2.8	5.8	17.5	31.7	12.5	19.1
Ce^{3+}-mont.	78.9	96.8	21.2	28.6	4.1	7.2	28.4	37.9	19.1	25.6
Al^{3+}-mont.	72.3	89.3	15.0	23.1	2.9	6.1	22.0	30.3	15.5	21.2
Fe^{3+}-mont.	76.1	94.6	19.3	25.7	3.4	6.6	25.8	34.7	17.9	23.4
γ-Al_2O_3	2.8	4.9	1.1	1.9	0	0	1.2	2.3	0.9	1.5
SiO_2	0	0	0.9	1.2	0	0	0	0	0	0
None[a]	0	0	0	0	0	0	0	0	0	0
Filtrate[b]	0	0	0	0	0	0	0	0	0	0

Experimental conditions: ketone: methanol molar ratio, 1:10; catalysts amount, 50 mg; steady flow of dry nitrogen. Reactions were carried out at ambient temperature and atmospheric pressure.
[a] Without using catalyst.
[b] After the reaction over H,Ce–Y zeolite, the catalyst was separated by filtration and the filtrate obtained was used to examine the catalytic activity of the possible dissolved components of the catalyst.

Table 3
Results obtained in the acetalization of benzaldehyde, 4-methoxybenzaldehyde, and 4-nitrobenzaldehyde with methanol over different solid acid catalysts.

Catalyst	Aldehyde conversion (%)					
	Benzaldehyde		4-Methoxybenzaldehyde		4-Nitrobenzaldehyde	
	2 h	10 h	2 h	10 h	2 h	10 h
H–Y	18.7	31.7	10.4	16.7	57.1	70.5
Ce,H–Y	44.1	70.3	15.6	25.4	73.5	89.7
Ce,Na–Y	41.6	61.2	12.3	20.5	65.5	81.6
K-10 mont.	47.3	84.7	27.9	41.7	71.6	92.1
Ce^{3+}-mont.	49.1	90.5	33.2	45.9	79.9	98.7
Al^{3+}-mont.	46.3	85.1	28.0	42.6	73.2	93.4
Fe^{3+}-mont.	47.9	86.5	30.4	44.1	75.3	95.2
γ-Al_2O_3	2.7	4.2	>1	1.1	3.4	6.5
SiO_2	0	0	0	0	1.1	3.2
None [a]	0	0	0	0	0	0
Filtrate[b]	0	0	0	0	0	0

Experimental conditions are as in Table 2. Reactions were carried out at ambient temperature and atmospheric pressure.
[a] Without using catalyst.
[b] After the reaction over H,Ce–Y zeolite, the catalyst was separated by filtration and the filtrate obtained was used to examine the catalytic activity of the possible dissolved components of the catalyst.

Table 4
Catalytic performance of H–Y, Ce,H–Y zeolites, and K-10 mont. and Ce-mont. catalysts during the acetalization of cyclohexanone and 4-nitrobenzaldehyde after one to three regeneration cycles.[a]

Catalytic system	Fresh	I cycle	II cycle	III cycle
H–Y	43.6 (57.1)	42.3 (56.5)	40.9 (56.7)	40.1 (56.1)
Ce,H–Y	70.1 (73.5)	69.8 (73.0)	69.5 (73.0)	68.9 (72.4)
K-10 mont.	71.7 (71.6)	71.2 (70.9)	70.8 (70.1)	69.5 (68.9)
Ce^{3+}-mont.	78.9 (79.9)	78.5 (79.3)	77.7 (78.6)	76.8 (77.5)

[a] Values in parenthesis are the conversion (%) of 4-nitrobenzaldehyde at ambient reaction conditions. Reaction conditions are as described in Tables 3 and 4 respectively.
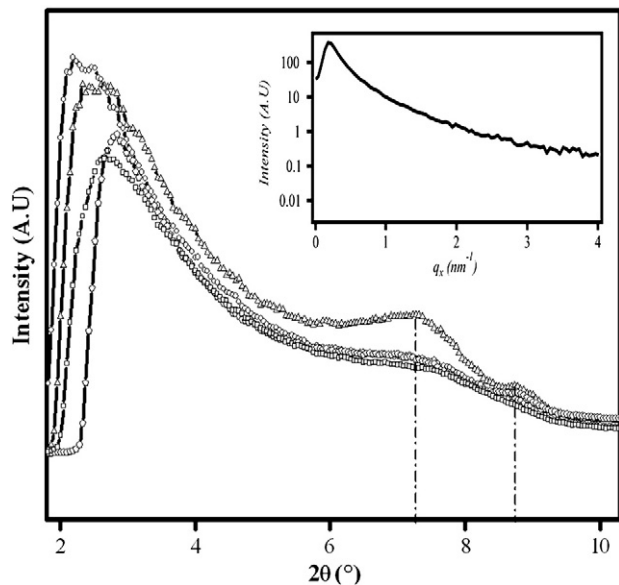
Fig. 1. Wide-angle X-ray scattering patterns of montmorillonite catalysts; (□) K-10 mont., (o) Ce−mont., (△) Fe-mont., and (Δ) Al-mont. Inset: small angle X-ray scattering pattern of K-10 mont.
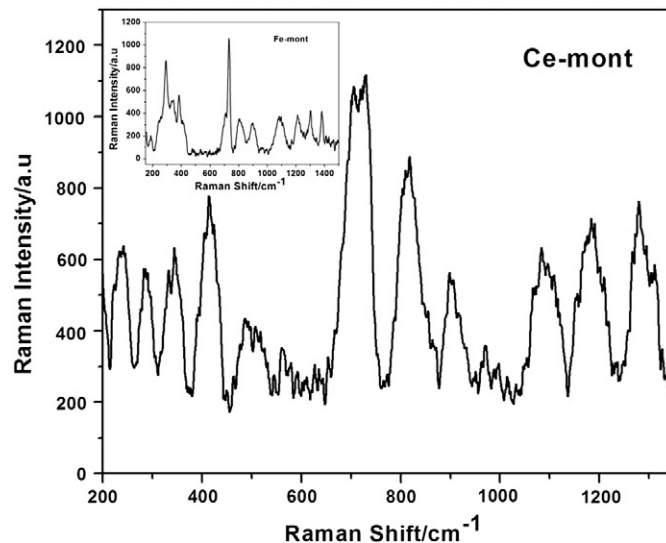

Fig. 2. Raman measurements of Ce-mont. in the spectral range of 200 to 1400 cm^{-1}. The inset shows the Raman spectrum of Fe-mont. in the same spectral range.
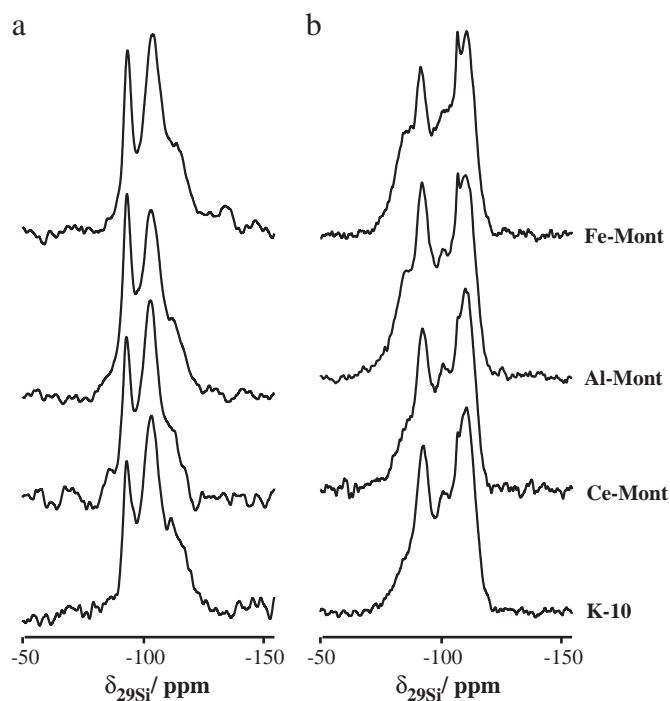

Fig. 3. (a) {^{1}H}–^{29}Si CP and (b) {^{1}H} ^{29}Si hpdec MAS NMR spectra of K-10 mont. and its cerium, aluminium and iron exchanged counterparts.
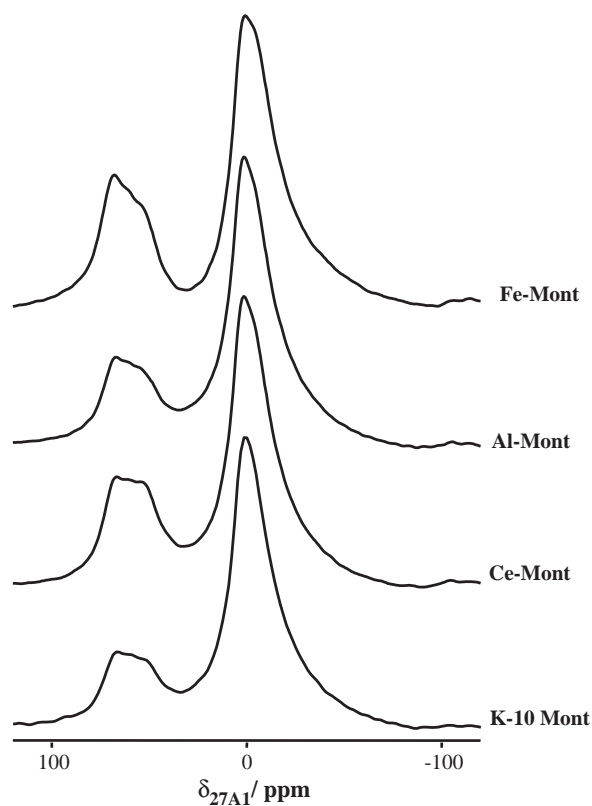
Fig. 4. ^{27}Al MAS NMR spectra of K-10 mont. and its cerium, aluminium and iron exchanged counterparts.
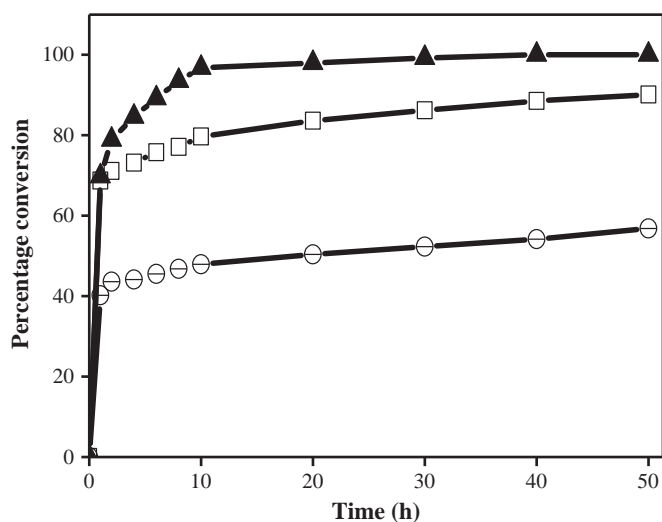
Fig. 5. The effect of the reaction time on the formation of 1,1-dimethoxycyclohexane with methanol over H–Y (Θ), Ce,H–Y (□) zeolites, and Ce-mont. (▲). Experimental conditions: cyclohexanone: methanol molar ratio, 1:10; ambient temperature and pressure; catalyst amount, 50 mg; steady flow of dry nitrogen.

Catalytic acetalization of carbonyl compounds over Ce³⁺, Fe³⁺ and Al³⁺ exchanged montmorillonites and Ce³⁺ exchanged Y zeolites

Bejoy Thomas[a,b*], Vasanthakumar Ganga Ramu[c], Sanjay Gopinath[a], Jino George[a], Manju Kurian[d], Guillaume Laurent[b], Glenna Drisko[b] and Sankaran Sugunan[a]

[a]*Department of Applied Chemistry, Cochin University of Science and Technology, Kochi-682 022, India.*

[b]*University Pierre et Marie Curie - Univ. Paris 06, CNRS, Laboratoire de Chimie de la Matière Condensée de Paris, Collège de France, 11 place Marcellin Berthelot, 75005 Paris, France.*

[c]*Organic Chemistry I, Faculty of Chemistry and Biochemistry, Ruhr-Universität Bochum, D-44780 Bochum, Germany.*

[d]*Mahatma Gandhi University Research Centre, Mar Athanasius College, Kothamangalam- 686 666 India.*
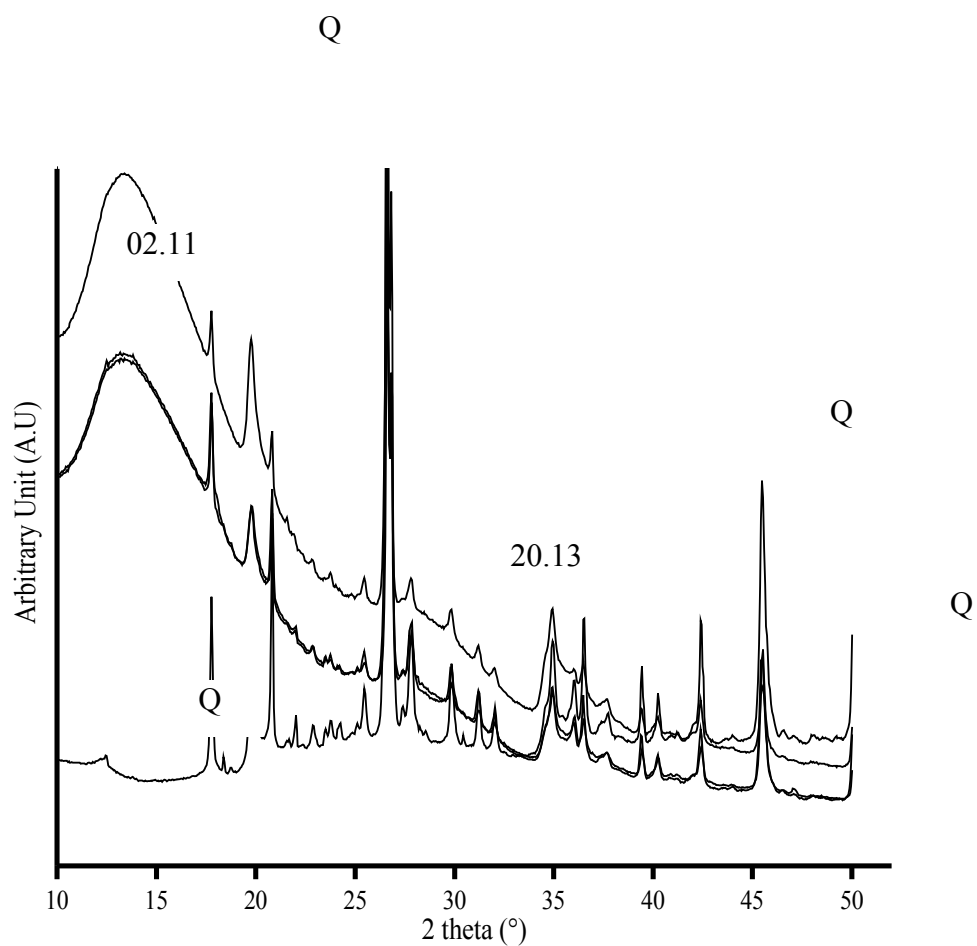
Figure SI. Powder X-ray diffraction patterns of activated K-10 mont. and its cation-exchanged counterparts. From top to bottom, K-10 mont., Al-mont., Ce-mont. and Fe-mont.

Table S1: [29]Si chemical shifts and the corresponding percentages of K-10 mont. and its cation exchanged counterparts as obtained from the deconvolution of high-power decoupling MAS and CP MAS NMR spectra.

Material	Percentages of various chemical shifts[a]							
	-75.0	-81.0	-86.0	-91.4	-93.0	-101.0	-107.1	-110.6
K-10 mont.	0.95	2.66	7.30	2.41	20.20	24.39	0.93	41.16
	(0.0)	(0.0)	(0.0)	(22.05)	(0.0)	(57.69)	(0.0)	(20.26)
Al-mont.	2.28	4.81	11.99	3.38	18.91	22.67	2.05	33.91
	(0.0)	(0.0)	(1.17)	(33.46)	(0.0)	(53.48)	(0.0)	(11.89)
Ce-mont.	1.06	2.78	8.2	2.50	19.17	25.69	0.67	39.93
	(0.0)	(0.0)	(0.36)	(27.72)	(0.0)	(61.50)	(0.0)	(10.41)
Fe-mont.	1.28	5.06	12.40	5.96	13.61	23.77	2.02	35.89
	(0.0)	(0.0)	(0.0)	(30.03)	(0.0)	(54.99)	(0.0)	(14.98)

[a.] Chemical shifts are in parts per million (ppm).

Values in parenthesis are the percentages of the silicon units obtained from the deconvolution of the CP MAS NMR spectra.
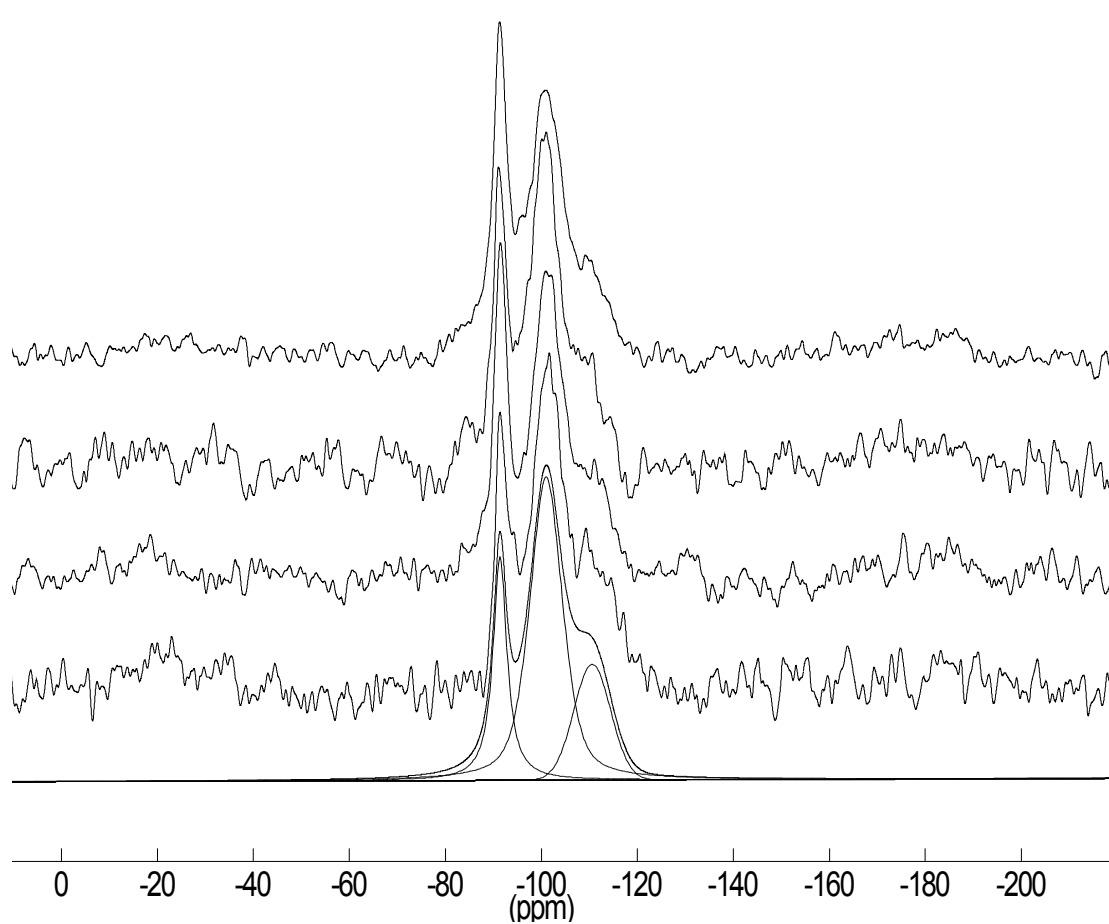
Figure S2. Deconvolution of ^{29}Si CP MAS NMR spectra of K10-mont. and its cation exchanged counterparts. From top to bottom from, Al-mont., Ce-mont., Fe-mont., K-10 mont. The deconvolution shown is for the K10-mont. System.
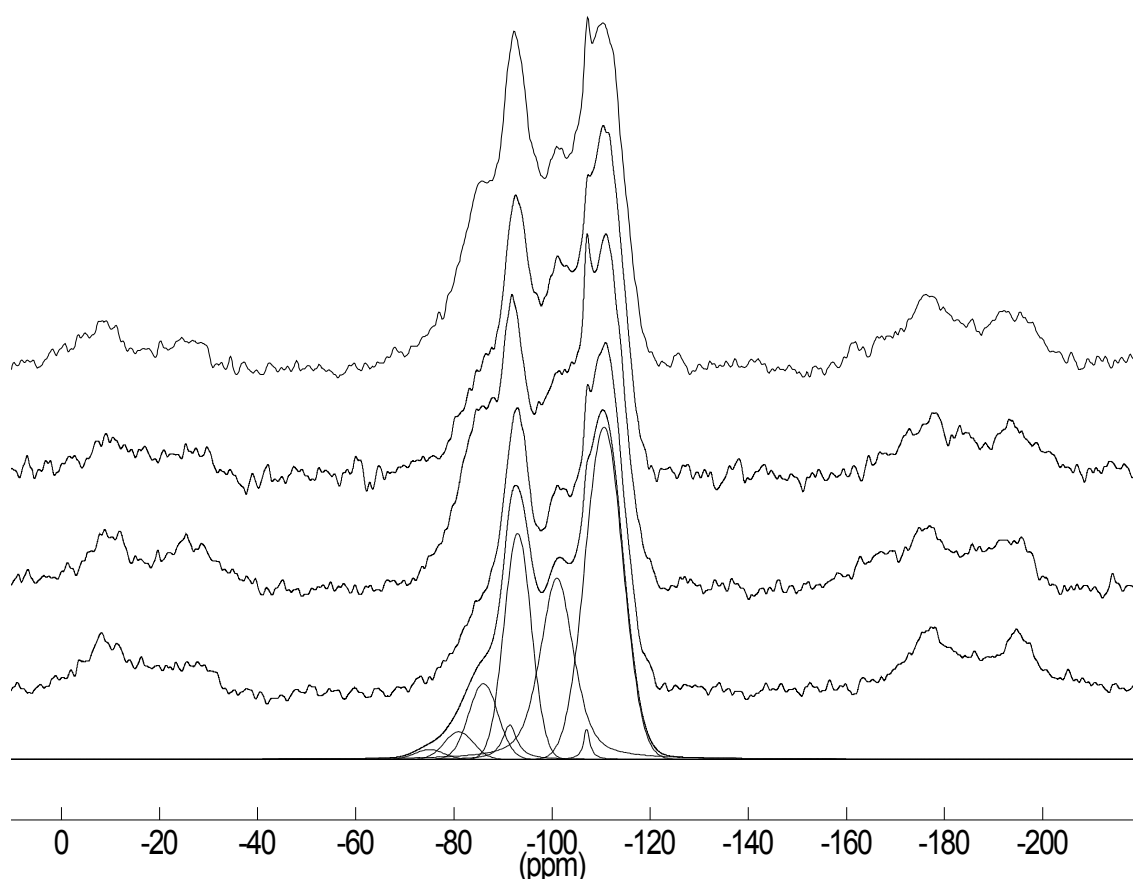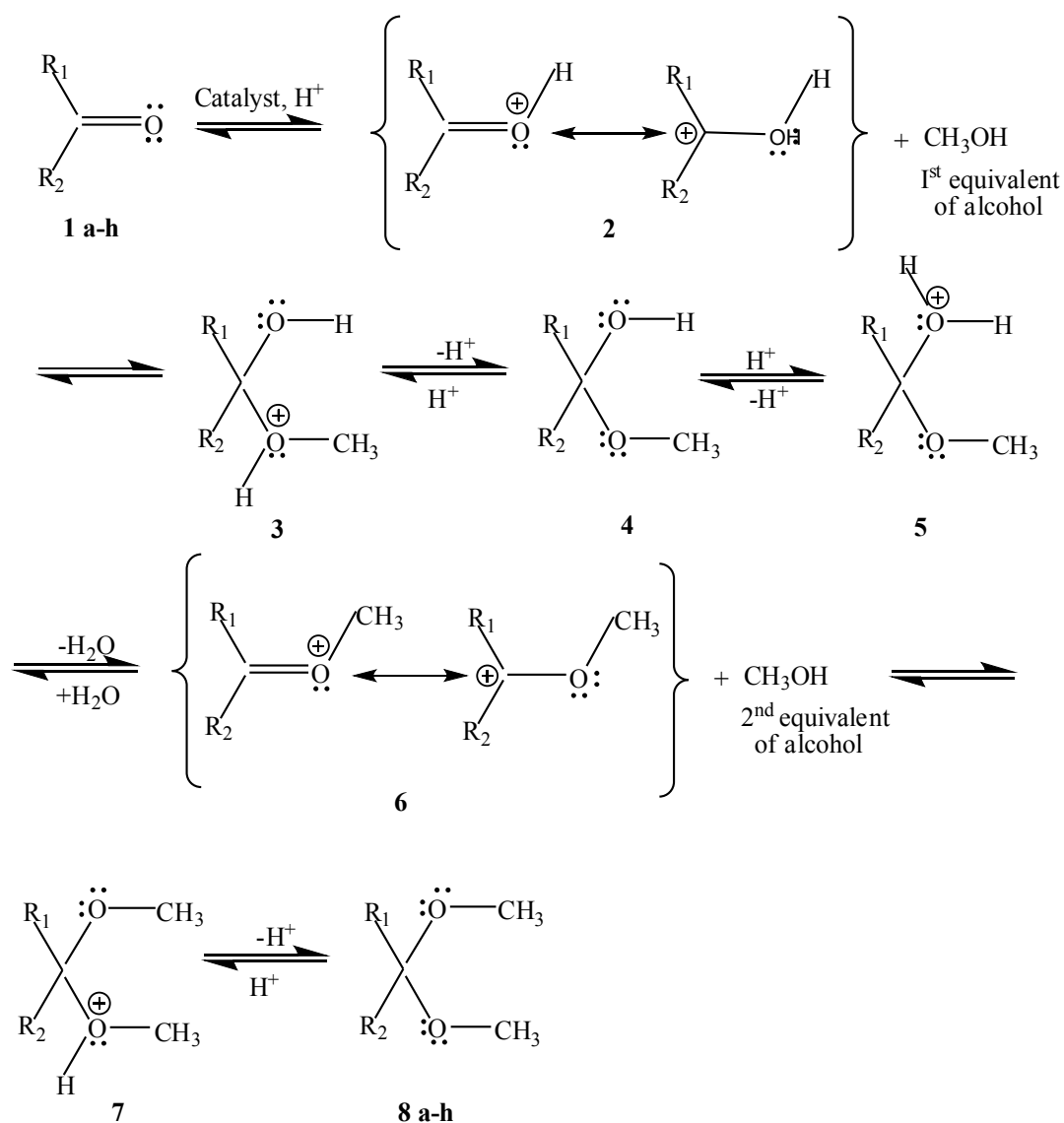
Figure S3. Deconvolution of ^{29}Si high-power decupling MAS NMR spectra of K10-mont. and its cation exchanged counterparts. From top to bottom Al-mont., Ce-mont., Fe-mont., K-10 mont. The deconvolution shown is for the K10-mont. system.

Reaction mechanism of acetalization

The first step in the acetalization reaction of aldehydes and ketones (**1a-h**) is an acid-base proton transfer, i.e., the oxygen of the carbonyl functionality is protonated by the Brönsted acid sites of the catalyst to produce the intermediate **2**, an electrophile. The second step is the nucleophilic attack by a methanol molecule to form a new ether bond (**2**). In the third step deprotonation of the methoxy ether oxonium ion produces the hemiacetal intermediate (**4**). Protonation of the alcohol creates a better leaving group. In the first step of an S_N1 substitution reaction a molecule of water is lost and a carbocation intermediate is formed (**6**). This carbocation intermediate is an analog of the protonated carbonyl seen in the first step of the process. A second molecule of the alcohol attacks the electrophilic carbon forming another trivalent oxygen intermediate (**7**). Finally, deprotonation of the oxonium produces an acetal (**8a-h**) and regenerates the acid catalyst. The formation of a carbocation (**6**) from the protonated hemiacetal (**5**) is the rate-determining step of the acetalization reactions. However, the hydroxyl protonation of the hemiacetal is also a slow step and the reaction medium has to be sufficiently acidic to promote efficient reaction rates. The reaction medium must be polar enough to stabilize the cation intermediates.

Scheme S1. Scheme showing a general depiction of the reaction mechanism for the acetalization of aldehydes and ketones with methanol in the presence of solid acid catalysts.
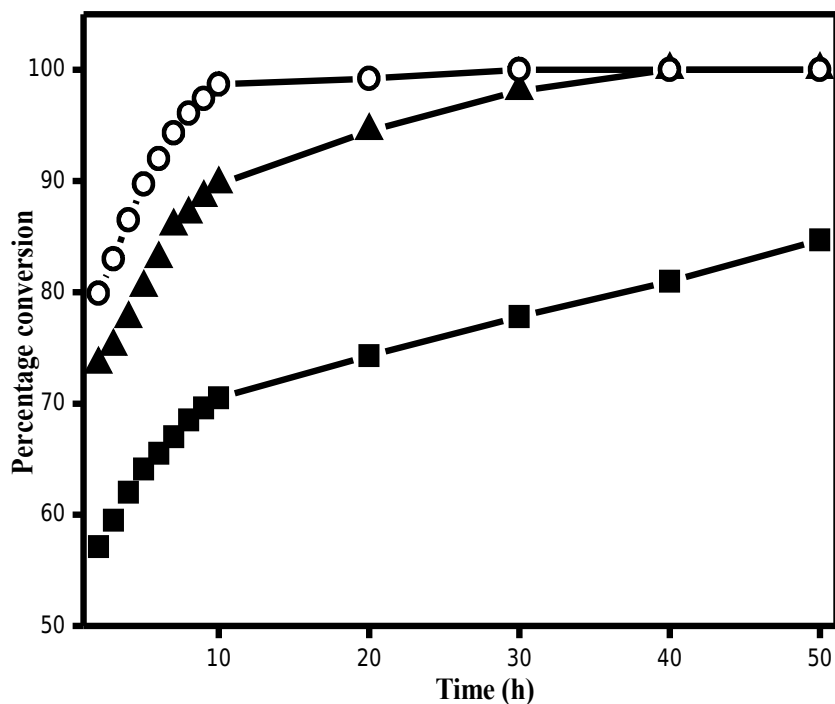
Compound (8)	R₁	R₂	Compound (8)	R₁	R₂
a	C_6H_5	C_6H_5	f	$C_6H_4NO_2$	H
b	C_6H_5	CH_3	g	$C_6H_4OCH_3$	H
c	$C_6H_4OCH_3$	H	h	C_6H_5	H
d	$C_6H_4NO_2$	H			
e	R_1-R_2 = C_5H_{10}				

Figure S4. The effect of reaction time on the formation of 1,1-dimethoxy-4-nitrobenzaldehyde with methanol over H-Y (-■-), Ce,H–Y (-▲-) zeolites, and cerium exchanged mont. (-○-). Experimental conditions: 4-nitrobenzaldehyde: methanol molar ratio, 1:10; ambient temperature and pressure; catalyst amount, 50 mg; steady flow of dry nitrogen.